JCI The Journal of Clinical Investigation

RIP140 increases *APC* expression and controls intestinal homeostasis and tumorigenesis

Marion Lapierre, … , Malcolm Parker, Vincent Cavailles

J Clin Invest. 2014;124(5):1899-1913. https://doi.org/10.1172/JCI65178.

Research Article **Oncology**

Deregulation of the Wnt/APC/β-catenin signaling pathway is an important consequence of tumor suppressor *APC* dysfunction. Genetic and molecular data have established that disruption of this pathway contributes to the development of colorectal cancer. Here, we demonstrate that the transcriptional coregulator RIP140 regulates intestinal homeostasis and tumorigenesis. Using *Rip140*-null mice and mice overexpressing human *RIP140*, we found that RIP140 inhibited intestinal epithelial cell proliferation and apoptosis. Interestingly, following whole-body irradiation, mice lacking RIP140 exhibited improved regenerative capacity in the intestine, while mice overexpressing RIP140 displayed reduced recovery. Enhanced RIP140 expression strongly repressed human colon cancer cell proliferation in vitro and after grafting onto nude mice. Moreover, in murine tissues and human cancer cells, RIP140 stimulated *APC* transcription and inhibited β-catenin activation and target gene expression. Finally, *RIP140* mRNA and RIP140 protein levels were decreased in human colon cancers compared with those in normal mucosal tissue, and low levels of *RIP140* expression in adenocarcinomas from patients correlated with poor prognosis. Together, these results support a tumor suppressor role for RIP140 in colon cancer.

RIP140 increases *APC* expression and controls intestinal homeostasis and tumorigenesis

Marion Lapierre,[1] Sandrine Bonnet,[1] Caroline Bascoul-Mollevi,[2] Imade Ait-Arsa,[1] Stéphan Jalaguier,[1] Maguy Del Rio,[1] Michela Plateroti,[3] Paul Roepman,[4] Marc Ychou,[5] Julie Pannequin,[6] Frédéric Hollande,[6] Malcolm Parker,[7] and Vincent Cavailles[1]

[1]IRCM, Institut de Recherche en Cancérologie de Montpellier, INSERM U896, Université Montpellier1, Montpellier, France. [2]Institut régional du Cancer Montpellier, Unité de Biostatistique, Montpellier, France. [3]Centre de Génétique et de Physiologie Moléculaire et Cellulaire, Université Lyon 1, CNRS, Villeurbanne, France. [4]Agendia NV, Amsterdam, The Netherlands, and Agendia Inc., Irvine, California, USA. [5]Institut régional du Cancer Montpellier, Service d'Oncologie Digestive, Montpellier, France. [6]Centre National de la Recherche Scientifique (CNRS), Unité Mixte de Recherche (UMR) 5203, Institut de Génomique Fonctionnelle, Montpellier, France. [7]Institute of Reproductive and Developmental Biology, Faculty of Medicine, Imperial College, London, United Kingdom.

Deregulation of the Wnt/APC/β-catenin signaling pathway is an important consequence of tumor suppressor *APC* dysfunction. Genetic and molecular data have established that disruption of this pathway contributes to the development of colorectal cancer. Here, we demonstrate that the transcriptional coregulator RIP140 regulates intestinal homeostasis and tumorigenesis. Using *Rip140*-null mice and mice overexpressing human *RIP140*, we found that RIP140 inhibited intestinal epithelial cell proliferation and apoptosis. Interestingly, following whole-body irradiation, mice lacking RIP140 exhibited improved regenerative capacity in the intestine, while mice overexpressing RIP140 displayed reduced recovery. Enhanced RIP140 expression strongly repressed human colon cancer cell proliferation in vitro and after grafting onto nude mice. Moreover, in murine tissues and human cancer cells, RIP140 stimulated *APC* transcription and inhibited β-catenin activation and target gene expression. Finally, *RIP140* mRNA and RIP140 protein levels were decreased in human colon cancers compared with those in normal mucosal tissue, and low levels of *RIP140* expression in adenocarcinomas from patients correlated with poor prognosis. Together, these results support a tumor suppressor role for RIP140 in colon cancer.

Introduction

The Wnt pathway is one of the major pathways deregulated in colorectal cancer. In the physiologically normal gut, activation of this pathway ensures proliferation of precursor cells and renewal of the intestinal epithelium by activating the transcriptional properties of the T cell factor/lymphoid enhancer factor-1 (TCF/LEF1) family (1). Stimulation by Wnt ligands leads to stabilization of the transcription coactivator β-catenin, which becomes associated with TCF/LEF1 in the nucleus, leading to the expression of specific target genes. Canonical Wnt signaling operates by regulating the phosphorylation and degradation of β-catenin (2). Without stimulation by Wnt ligands, the levels of β-catenin in the cytoplasm are normally regulated by a multiprotein destruction complex that targets for degradation. This complex is assembled over the scaffold component axin, which contains binding domains for β-catenin, the tumor suppressor adenomatous polyposis coli (APC), and glycogen synthase kinase-3 (GSK3) and casein kinase 1 (CSNK1). Within the axin complex, β-catenin is sequentially phosphorylated by CSNK1 and GSK3 and then degraded by the proteasome (3). This complex thereby controls the proliferation of intestinal epithelial cells by maintaining the pool of active β-catenin. However, mutations of the *APC* gene, which were first identified in patients suffering from familial adenomatous polyposis (FAP), occur in a high proportion of sporadic colorectal carcinomas (up to 80%) (4). Stimulation of the Wnt pathway due to a mutation in the negative regulator APC provokes the hyperproliferation of the epithelium. Several mouse models have been generated, such as the $Apc^{\Delta 14/+}$ mouse, in which exon 14 has been deleted (frameshift mutation at codon 580) and which presents a FAP phenotype with tumors in the distal colon and rectum, showing that heterozygous disruption of the *Apc* gene is associated with accumulation of β-catenin and overexpression of the β-catenin target genes cyclin D1 and c-Myc (5).

The transcription cofactor RIP140 (receptor-interacting protein of 140 kDa), also known as NRIP1 (nuclear receptor–interacting protein 1), was first identified in human cancer cells through its interaction with estrogen receptor α (6). RIP140 was also shown to interact with many other nuclear receptors (NRs) and transcription factors (for a review see ref. 7). More recently, we demonstrated that RIP140 behaves as an Rb-like regulator of the E2F pathway by directly binding to E2Fs and repressing their transactivation potentials (8). RIP140 mainly acts as a transcriptional repressor by means of four inhibitory domains that recruit histone deacetylases or C-terminal binding proteins (9). Several post-translational modifications, such as sumoylation and acetylation, also play important roles in controlling the subcellular location and repressive activity of RIP140 (for a review see ref. 10). *RIP140* is a ubiquitously expressed gene whose transcription is finely regulated at the transcriptional levels by both NRs and E2Fs (11). The physiological importance of RIP140 has been evaluated using mice

Conflict of interest: The authors have declared that no conflict of interest exists.
Citation for this article: *J Clin Invest.* 2014;124(5):1899–1913. doi:10.1172/JCI65178.

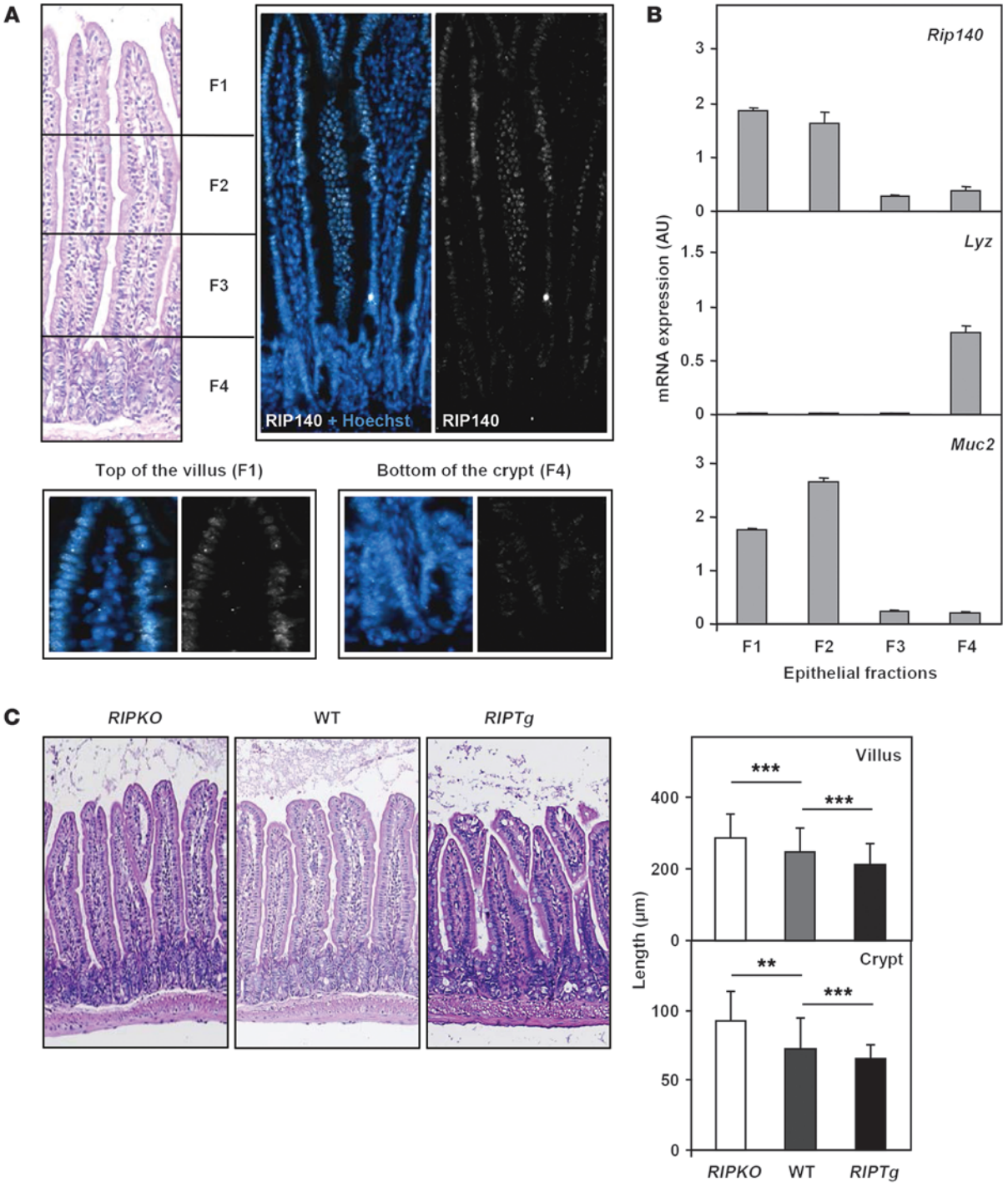

Figure 1

RIP140 expression in mouse intestinal epithelium. (**A**) Immunofluorescence showing a gradient of RIP140 in the nuclei of epithelial cells along the villus/crypt axis of wild-type mice. Original magnification, ×20. (**B**) Real-time qPCR analysis of *Rip140* mRNA in wild-type intestinal epithelial fractions. mRNAs encoded by the *Lyz* and *Muc2* genes were used to verify the enrichment in villus- or crypt-associated cells. Data were normalized to *RS9* mRNA. mRNA quantification for each gene is indicated in AU as the mean ± SD; $n = 4$ mice. (**C**) Left panel: H&E-stained transverse sections of small intestine from *RIPKO*, wild-type, and *RIPTg* mice. Right panel: The length of villi and crypts was measured on at least six fields selected from whole intestine sections of each mouse of the three different genotypes. Values represent the means ± SD; $n = 6$ mice for each genotype. Original magnification, ×10. Mann-Whitney *U* test. $^{**}P < 0.01$; $^{***}P < 0.001$.

that lack the *Rip140* gene (*RIPKO* mice). These animals are viable, but display a wide range of phenotypic alterations in various tissues and organs such as infertility of female mice (12) or reduced body fat content (13), and, more recently, severe cognitive impairments (14) and mammary gland morphogenesis (15).

Our present results demonstrate the role of RIP140 in homeostasis and tumorigenesis of the intestinal epithelium. We used mice with a loss or gain of RIP140 function to show that RIP140 inhibits cell proliferation and apoptosis in the intestinal epithelium. At the molecular level, RIP140 positively controls *APC* gene expression and, consequently, reduces β-catenin activation and Wnt target gene expression. Overexpression of RIP140 inhibits the proliferation of human colon cancer cells in vitro and in vivo after grafting onto nude mice. Finally, RIP140 mRNA and protein levels are reduced in colon cancer biopsies as compared with those in normal tissue, and patients whose tumors exhibit high *RIP140* gene expression have the best survival rates. Altogether, this work identifies RIP140 as a key factor regulating intestinal tumorigenesis and as a potential new oncology biomarker.

Results

RIP140 expression in the intestinal epithelium. Previous data indicated that RIP140 is a ubiquitously expressed transcription factor (16). By quantitative real-time quantitative PCR (qPCR) analysis, *Rip140* mRNA was detected in all the mouse tissues tested and particularly in the intestine and colon (Supplemental Figure 1A; supplemental material available online with this article; doi:10.1172/JCI65178DS1). First, we used immunofluorescence to analyze the distribution of RIP140 in the intestinal epithelium of wild-type mice and found that RIP140 was expressed in the nucleus of all epithelial intestinal cells, with a clearly increasing gradient along the crypt/villus axis (Figure 1A). To confirm this observation, we applied sequential isolation of wild-type mouse small intestine epithelial cells. To verify the enrichment of the different fractions in villus-associated or crypt-associated cells, we quantified the mRNA levels of the lysozyme (*Lyz)* and mucin 2 (*Muc2*) genes, which are, respectively, differentiation markers of Paneth cells located in the crypts and goblet cells in the villi (17). As expected, the *Lyz* gene was exclusively expressed in cells from fraction 4, whereas the *Muc2* gene was mainly expressed in cells from fractions 1 and 2 (Figure 1B). Using the same enriched fractions, we found that the expression of *Rip140* mRNA was significantly higher in differentiated cells of the villi than in cells from the crypts (Figure 1B).

RIP140 alters small intestine homeostasis. To study the role of RIP140 in the intestinal epithelium, we used *Rip140*-null (*RIPKO*) or *RIP140* transgenic (*RIPTg*) mice. In these two mouse models, the respective deletion and overexpression of the *Rip140* gene in intestinal sections were validated by immunofluorescence (Supplemental Figure 1B). As expected, RIP140 protein was undetectable in the *RIPKO* mice and overexpressed in the nuclei of all intestinal epithelial cells in the *RIPTg* mice as compared with their wild-type littermates. Real-time qPCR analysis confirmed that *RIPKO* mice expressed β-galactosidase as a marker of murine *Rip140* gene disruption (12) and that the transgenic human *RIP140* gene was specifically expressed in *RIPTg* mice (Supplemental Figure 1C).

Qualitative histopathological analysis of paraffin sections stained with hematoxylin and eosin (H&E) demonstrated no gross morphological changes in the structures of the intestinal epithelia of the two mouse models (Figure 1C, left panel). However, precise measurements of villus and crypt lengths demonstrated statistically significant differences between transgenic and wild-type animals (Figure 1C, right panel). Indeed, when compared with wild-type animals, the length of the crypt/villus axis increased in *Rip140*-null mice and decreased in mice overexpressing RIP140. This was associated with an altered total length of the small intestine, which was shorter in *RIPKO* mice and longer in *RIPTg* animals when compared with their respective wild-type littermates (Supplemental Figure 1D, top panel). As a consequence, invalidation or overexpression of the *Rip140* gene did not affect the total surface area of the intestinal epithelium (Supplemental Figure 1D, bottom panel).

RIP140 inhibits cell proliferation and apoptosis. To determine whether cell proliferation was regulated by RIP140 expression, mice were injected with 5-ethynyl-2′-deoxyuridine (EdU) 2 hours prior to sacrifice. As shown in Figure 2A, analysis of EdU labeling demonstrated that the number of cells synthesizing DNA was significantly increased (2.6-fold) in *RIPKO* mice as compared with that in wild-type animals. By contrast, the level of EdU staining decreased (3.7-fold) in *RIPTg* mice as compared with that seen in control mice. These results were strengthened by quantifying the mRNAs corresponding to *Myc* and proliferating cell nuclear antigen (*Pcna*) genes (Supplemental Figure 2A). The corresponding mRNA levels were increased up to 2-fold in *RIPKO* mice and were decreased by up to 3-fold in the *RIPTg* strain as compared with mRNA levels in the wild-type animals. The differences in *Pcna* gene expression among the three genotypes were confirmed by immunofluorescence labeling (Supplemental Figure 2B). We next assessed the effect of RIP140 expression on apoptosis by TUNEL assay on intestinal sections. The top of the villi showed a significant 3-fold increase in TUNEL-positive cells in *Rip140*-null mice as compared with that observed in their wild-type littermates, whereas villi overexpressing RIP140 (*RIPTg*) showed a clear 2-fold decrease in apoptosis (Figure 2B). Altogether, these observations suggest that RIP140 regulates both cell proliferation and apoptosis and may therefore inhibit the renewal of intestinal epithelium.

RIP140 inhibits the response of intestinal epithelium to irradiation. To highlight the role of RIP140 in the homeostasis of intestinal mucosa, *RIPKO* and *RIPTg* mice, together with their wild-type littermates, were exposed to a single 12-Gy dose of whole-body irradiation (WBI). On day 2.5, a time when recovery begins, we assessed the number and length of villi together with the length of crypts after H&E staining of intestinal paraffin sections (Figure 2C). Following WBI, we observed that *Rip140*-null mice exhibited a significantly increased number of regenerating villi as compared with that seen in wild-type animals. The length of villi and crypts was also significantly higher in *RIPKO* animals. As shown in Supplemental Figure 2C, this effect was associated with a strong rise in PCNA staining in the crypts, where progenitors and stem cells reside, and suggested a role for RIP140 in ionizing radiation–induced cell proliferation. As expected, this process was much slower in *RIPTg* mice (Figure 2C), which exhibited only a few buds of villi and weak PCNA staining of crypt cells 2.5 days after WBI (Supplemental Figure 2C). Altogether, these results strongly indicate that RIP140 inhibits renewal of the intestinal epithelium.

RIP140 controls β-catenin activation. Wnt/APC/β-catenin signaling is the major pathway regulating cellular homeostasis of the intestinal epithelium (18). To decipher the underlying mechanisms involved in the effect of RIP140 in intestinal epithelium homeostasis, we sought to establish whether its expression impacted the Wnt/APC/β-catenin signaling pathway. We first investigated the pattern of β-catenin expression and activity in the intestinal

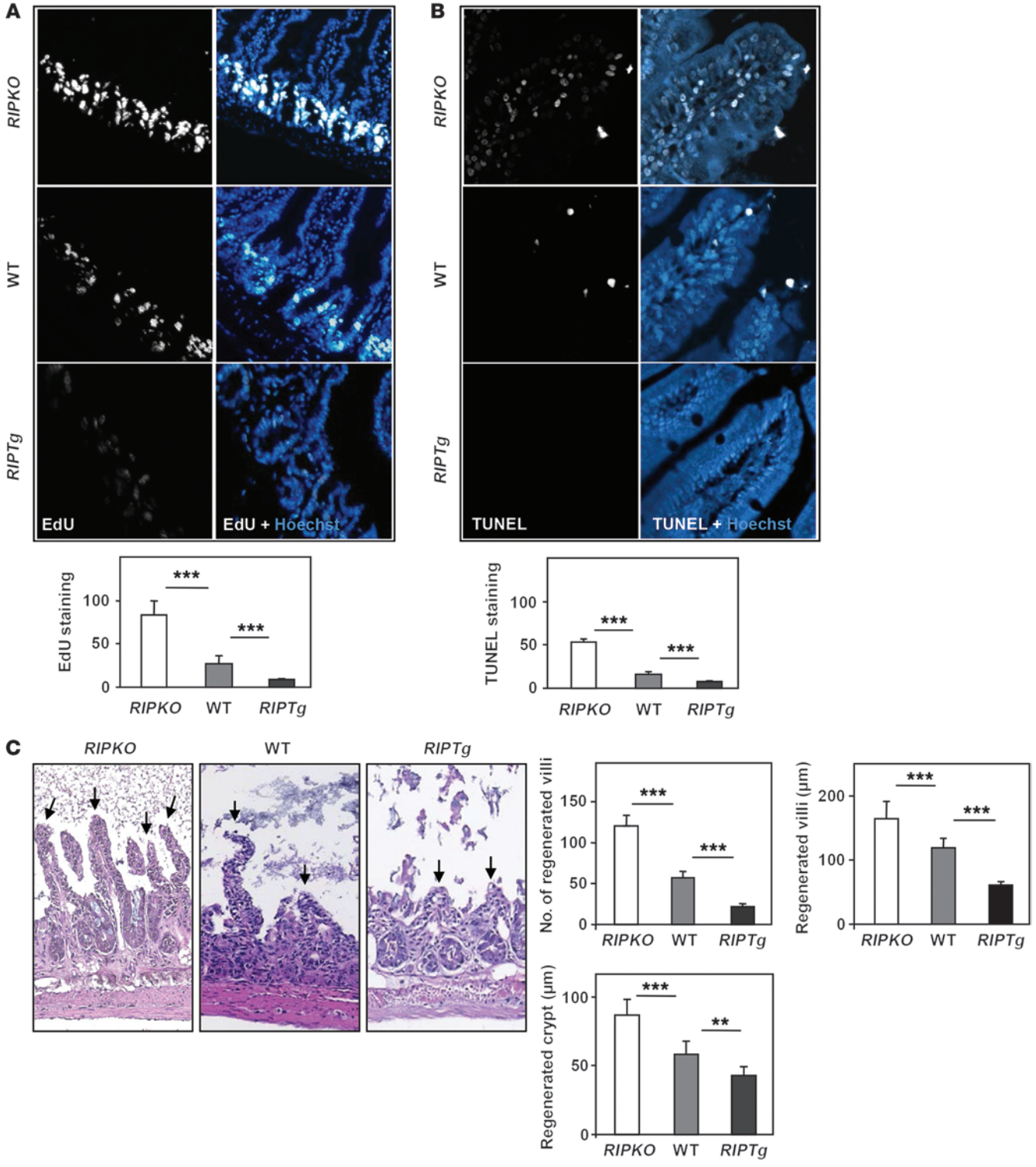

Figure 2

RIP140 inhibits intestinal cell proliferation and apoptosis. (**A**) EdU labeling of proliferating cells or (**B**) TUNEL staining in paraffin sections of small intestine from *RIPKO*, wild-type, and *RIPTg* mice. Images show merged EdU or TUNEL detection (white) and nuclear staining (blue) in small intestine. Staining is expressed as the means of signal quantification ± SD; $n = 6$ mice for each genotype. Original magnification, ×20 (**A**) and ×40 (**B**). (**C**) Representative H&E-stained transverse sections of small intestines showing crypt survival in irradiated mice (2.5 days after 12-Gy WBI). The number of surviving villi (indicated by black arrows) and the length of villi and crypts were counted in at least six fields of small intestine cross sections from *RIPKO*, wild-type, and *RIPTg* mice. Values are the means ± SD; $n = 6$ mice for each genotype. Original magnification, ×10. Mann-Whitney *U* test. $^{**}P < 0.01$; $^{***}P < 0.001$.

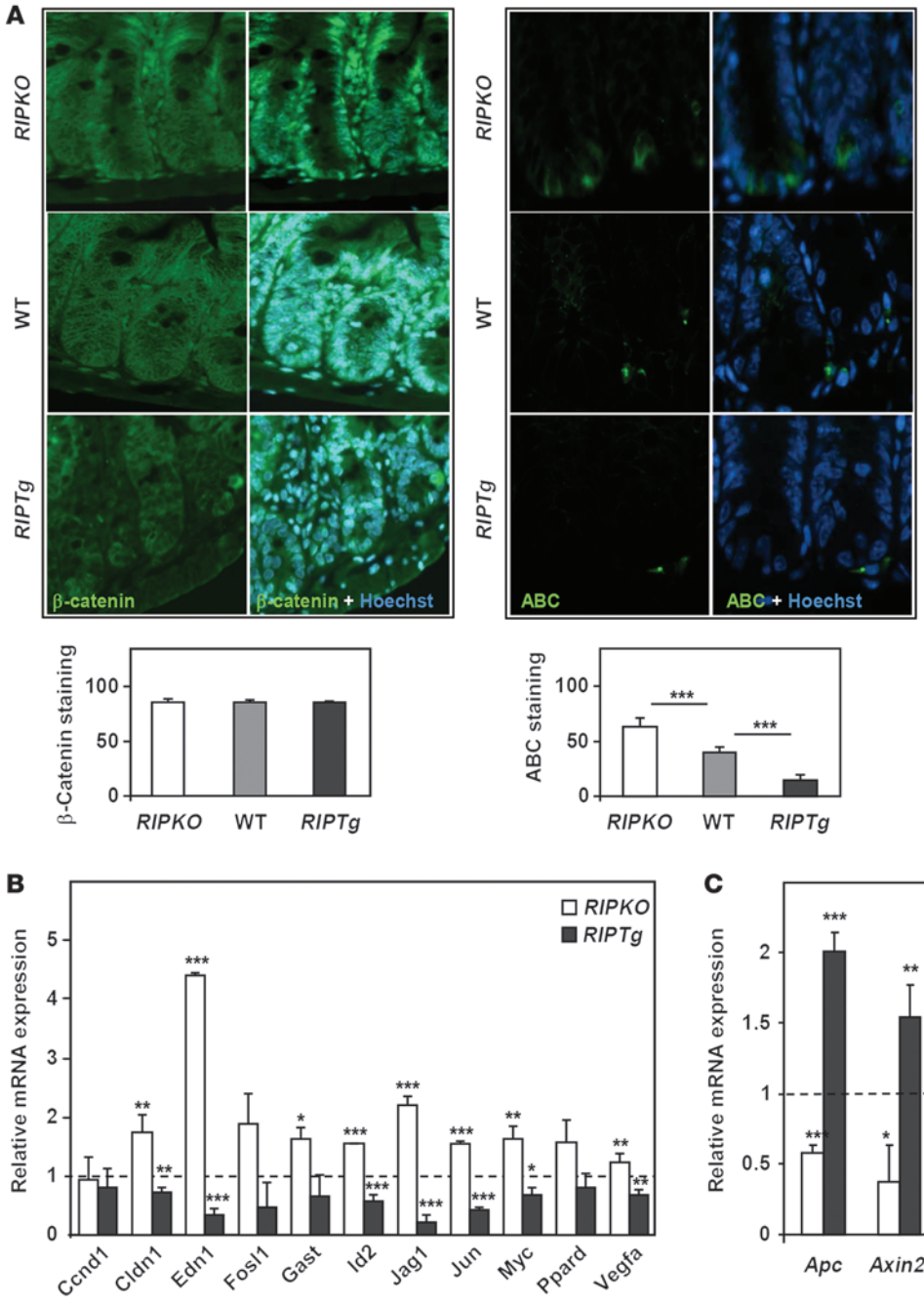

Figure 3

Activation of β-catenin by RIP140 in mouse intestinal epithelium. (**A**) Total (left panel) and active (right panel) β-catenin (ABC) in paraffin-embedded sections of small intestine from *RIPKO*, wild-type, and *RIPTg* mice (β-catenin immunolabeling in green and nuclear staining in blue). Values are the means ± SD; $n = 6$ mice for each genotype. Original magnification, ×40 (left panels) and ×63 (right panels). (**B**) Expression of β-catenin–regulated genes was measured by real-time qPCR analysis in *RIPKO*, wild-type, and *RIPTg* mice. Values represent fold change ± SD versus levels in wild-type mice after normalization to *RS9* mRNA; $n = 4$ mice for each genotype. (**C**) Same as in **B** for the expression of different members of the degradation complex. Mann-Whitney *U* test. $^{*}P < 0.05$; $^{**}P < 0.001$; $^{***}P < 0.001$.

epithelia of the different mutant mice (Figure 3A). Immunolabeling of paraffin sections of small intestine from *Rip140*-null and transgenic mice revealed no significant differences in the levels of total β-catenin (Figure 3A, left panel). We then measured the level of active β-catenin (which represents only a small fraction of total β-catenin; ref. 19) using an antibody specific to the protein dephosphorylated on Ser37 or Thr41. Quantification of active β-catenin (ABC) staining revealed clear regulation by RIP140, with a 2-fold increase in *RIPKO* mice and about a 3-fold decrease in *RIPTg* mice as compared with controls (Figure 3A, right panel). In order to validate the regulation of β-catenin activation by RIP140, we evaluated β-catenin transcriptional activity in intestinal epithelium by quantifying the mRNA levels of several target genes. As shown in Figure 3B, we observed a significant regulation of most of these genes (e.g., c-Myc [*Myc*]; claudin 1 [*Cldn1*], ref. 20; endothelin 1 [*Edn1*], ref. 21; jagged 1 [*Jag1*], ref. 22; and c-Jun [*Jun*], ref. 23), whose mRNA levels were increased in *Rip140*-null mice and reduced in *RIPTg* mice as compared with levels in wild-type animals. For endothelin 1 and jagged 1, the same deregulation was observed at the protein level by immunofluorescence (data not shown). Finally, since activation of the Wnt pathway drives the differentiation program of Paneth cells (24), we investigated the effect of RIP140 on this lineage. Using an antibody specifically directed against lysozyme, we observed that the number of Paneth

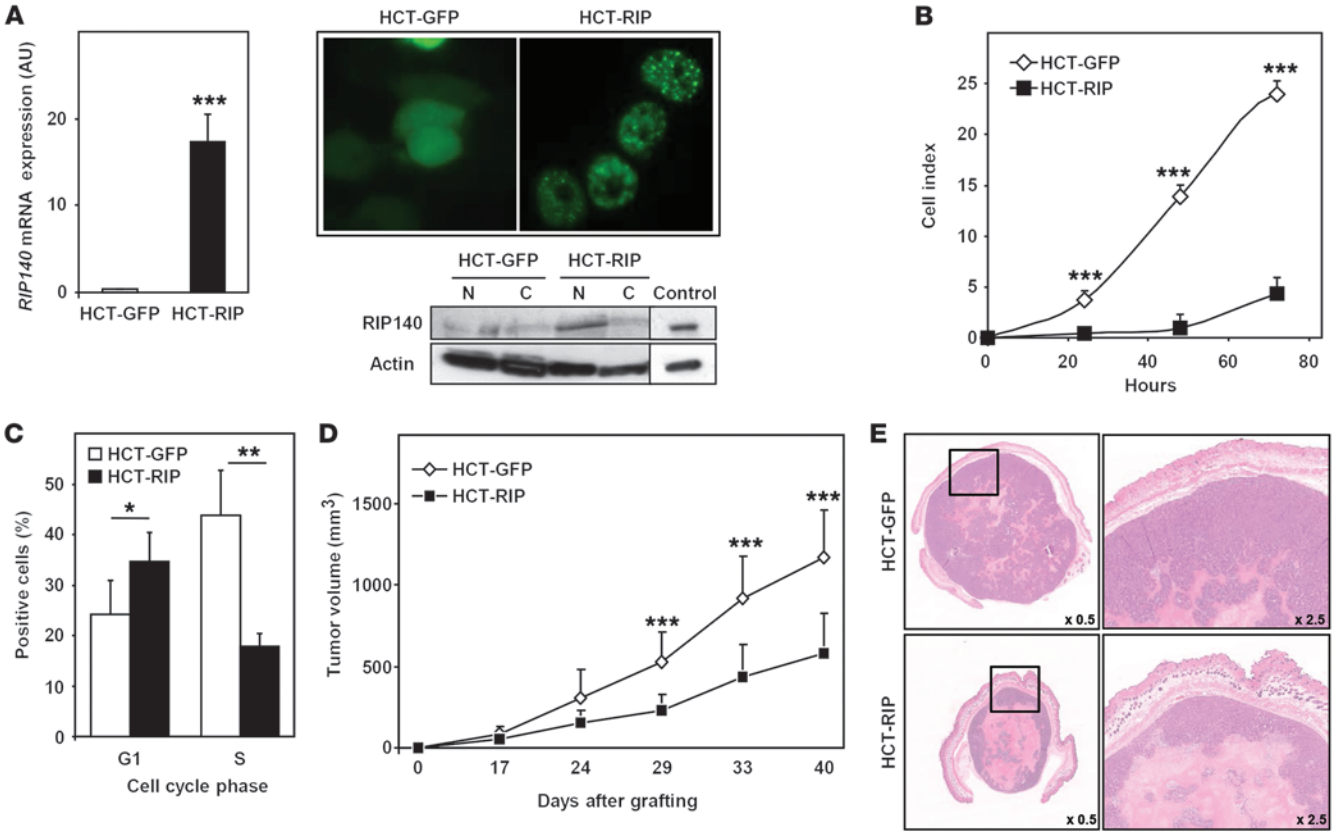

Figure 4
Effect of RIP140 on the proliferation of HCT116 human colon cancer cells. (**A**) Real-time qPCR analysis of HCT116 cells with or without overexpression of RIP140. Data are expressed in AU after normalization to *RS9* mRNA levels. Values are the means ± SD; $n = 5$ independent experiments. RIP140 protein levels were detected by Western blotting and immunofluorescence. Blot lanes were run on the same gel, but were noncontiguous. Original magnification, ×40. (**B**) Cell index corresponding to the number of HCT-GFP or HCT-RIP viable cells was measured every 24 hours for a total of 72 hours. (**C**) Percentages of HCT-GFP and HCT-RIP cells in G1 and S phases were determined in ten fields. Values are the means ± SD, normalized to the total number of cells; $n = 5$ independent experiments. (**D**) Volumes of HCT-GFP and HCT-RIP cell xenografts were measured at different times after grafting. Values are the means ± SD; $n = 12$ xenografts per cell line. (**E**) Representative necrotic areas observed in xenograft sections stained with H&E. Mann-Whitney test. $^*P < 0.05$; $^{**}P < 0.001$; $^{***}P < 0.001$. Original magnification, ×0.5 (left panels) and ×2.5 (right panels).

cells per crypt increased in *RIPKO* mice and decreased in *RIPTg* mice (Supplemental Figure 3), thus strengthening the negative regulation of the Wnt signaling pathway by RIP140.

RIP140 positively regulates Apc gene expression. ABC levels are normally controlled by a multiprotein degradation complex composed of APC, AXIN1 and 2, GSK3β, CSNK1, and PP2A (18). We therefore postulated that RIP140 could control the level of β-catenin activation by influencing the expression of members of this degradation complex. To test this hypothesis, we quantified the mRNAs encoded by the main genes implicated in β-catenin degradation. Interestingly, we found a correlation between expression of the *Rip140* gene and the mRNA levels of *Apc*, *Axin2*, and *Csk1E* genes, which were decreased and increased in *Rip140*-null and transgenic mice, respectively (Figure 3C). This suggests that RIP140 inhibits β-catenin activation in the intestinal epithelium by positively regulating the expression of several members of the β-catenin degradation complex. Altogether, this inhibition of the β-catenin signaling pathway could explain, at least in part, the above-described effects of RIP140 on intestinal homeostasis.

RIP140 inhibits proliferation of human colon cancer cells. Given the critical role played by the Wnt/APC/β-catenin pathway in promoting colon tumorigenesis, we then investigated the role of RIP140 in human colon cancer cells. First, we measured *RIP140* gene expression in different colorectal cancer cell lines by real-time qPCR and observed that the gene was much more weakly expressed in colon cancer cells than in breast cancer cell lines (data not shown). To analyze the effects of RIP140 on the malignant phenotype of human colon adenocarcinoma cells, we established a stably transfected HCT116 cell line overexpressing a GFP-tagged version of RIP140 (HCT-RIP cells) and used the same cells transfected with the pEGFP empty vector (HCT-GFP cells) as a control. Real-time qPCR analysis confirmed a much greater abundance of *RIP140* mRNA in the HCT-RIP cells compared with that in control HCT-GFP cells (Figure 4A, left panel). Similarly, Western blot analysis confirmed that GFP-RIP140 protein was overexpressed in the nuclear fraction of HCT-RIP cell lysates (Figure 4A, right panel). Fluorescence analysis of HCT-GFP and HCT-RIP cells revealed a cytoplasmic labeling corresponding to GFP-expressing cells and,

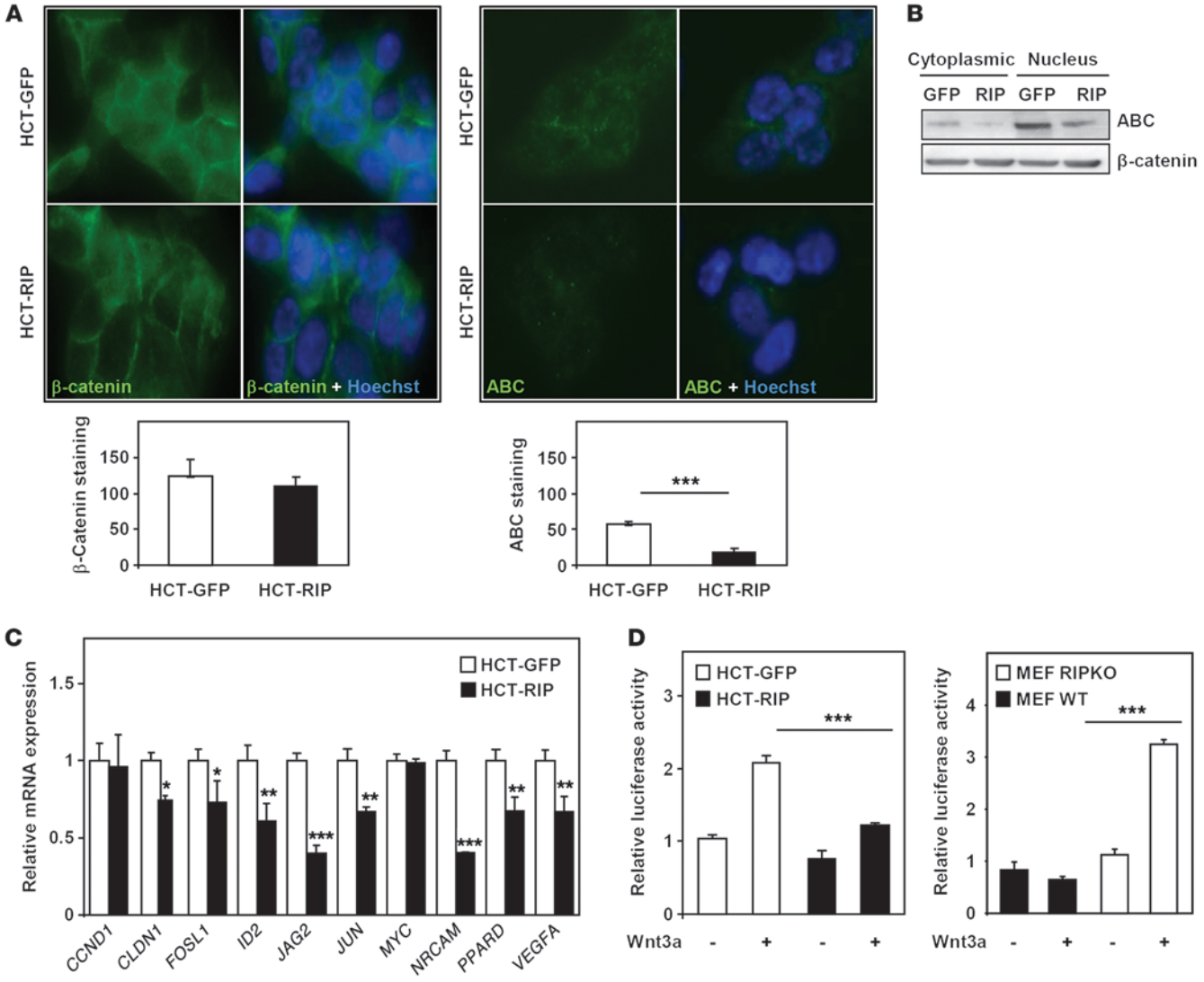

Figure 5

Regulation of β-catenin activation by RIP140 in HCT116 colon cancer cells. (**A**) Total (left panel) and active (right panel) β-catenin in HCT-GFP and HCT-RIP colon cancer cells (β-catenin immunolabeling in green and nuclear staining in blue). Quantifications are the means ± SD; $n = 6$ independent experiments for each cell line. Original magnification, ×63. (**B**) Levels of total and ABC proteins were detected by Western blot analysis using specific antibodies in HCT-GFP and HCT-RIP cells. (**C**) Expression of β-catenin–regulated genes was measured by real-time qPCR. Values represent fold changes ± SD corrected by *28S* mRNA and normalized to HCT-GFP cells; $n = 6$ independent experiments for each cell line. (**D**) TOP/FOP experiments were performed by transiently transfecting HCT-GFP and HCT-RIP cells (left panel) or MEF WT and MEF RIPKO cells (right panel) with the pTOPflash or pFOPflash reporter plasmids (200 ng). Cells were treated with or without Wnt3a-conditioned medium. Relative luciferase activity was expressed as the mean ratio of TOP/FOP luciferase activities ± SD; $n = 3$ independent experiments. Mann-Whitney *U* test. $^{*}P < 0.05$; $^{**}P < 0.001$; $^{***}P < 0.001$.

as expected, a punctuate signal corresponding to the previously described localization of GFP-RIP140 protein in speckles (ref. 25 and Figure 4A, right panel).

We first investigated the effect of RIP140 expression on cell proliferation using XCELLigence technology (Roche Diagnostics), which allows real-time monitoring of cell proliferation through measurement of impedance-based signals. Data shown in Figure 4B clearly demonstrate that RIP140 inhibited human colon cancer cell proliferation in vitro. To determine whether RIP140 affected cell cycle progression, we transiently transfected the two stable HCT116 cell lines with a cdt1-RFP Premo FUCCI Cell Cycle Sensor, allowing the detection of cells in G1. In parallel, we performed EdU labeling in order to monitor cells synthesizing DNA (Figure 4C). When compared with control cells, HCT-RIP cells showed a strong and significant decrease in the S-phase cell population (from 43.8% to 17.8%), with a concomitant increase in the number of cells in the G1 phase (from 24.1% to 34.6%). These data indicate that RIP140 expression results in a significant and specific blockade of cell cycle progression with cell arrest in G1.

We then assessed the impact of RIP140 on tumor growth in vivo by testing the ability of HCT-GFP and HCT-RIP cells grafted s.c. onto immunodeficient mice to form tumors (Figure 4D). In line

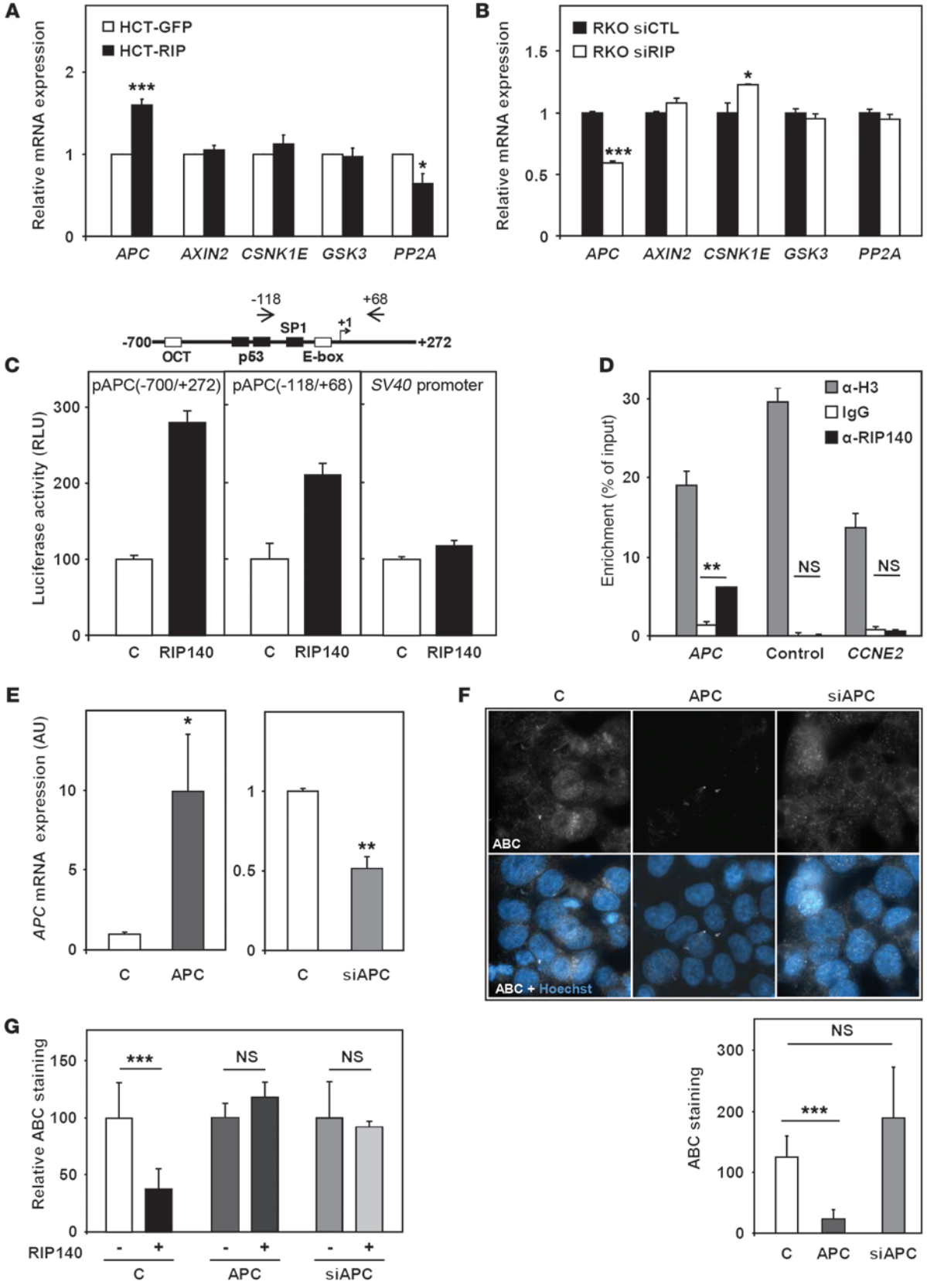
A
HCT-GFP
HCT-RIP
Relative mRNA expression
APC
AXIN2
CSNK1E
GSK3
PP2A
B
RKO siCTL
RKO siRIP
Relative mRNA expression
C
-118
+68
SP1
+1
-700
+272
OCT
p53
E-box
pAPC(-700/+272)
pAPC(-118/+68)
SV40 promoter
Luciferase activity (RLU)
C
RIP140
D
α-H3
IgG
α-RIP140
Enrichment (% of input)
Control
CCNE2
E
APC mRNA expression (AU)
siAPC
F
ABC
ABC + Hoechst
G
Relative ABC staining
ABC staining
NS

Figure 6
Regulation of *APC* gene transcription by RIP140 in human colon cancer cells. (**A**) Expression of members of the β-catenin degradation complex was measured by real-time qPCR. Values represent fold changes ± SD corrected by *28S* mRNA and normalized to HCT-GFP cells; $n = 6$ independent experiments. (**B**) Same as in **A** for RKO-siCTL and RKO-siRIP cells. (**C**) Schematic drawing of the human *APC* gene promoter region showing experimentally characterized transcription factor–binding sites. HCT116 cells were transfected with two different *APC* gene promoter reporter vectors or with an SV40-based reporter vector with or without a RIP140 expression vector. Relative luciferase activity was expressed as the means ± SD; $n = 3$ independent experiments. (**D**) ChIP experiments were performed on the *APC* gene proximal promoter, on an upstream region (Control), or on the *CCNE2* promoter after ChIP using an antibody against total histone H3, an antibody against RIP140, or an irrelevant antibody (IgG). (**E**) Expression of APC was measured by real-time qPCR after overexpression (APC) or silencing (siAPC) of the *APC* gene. Values represent fold changes ± SD corrected by *28S* mRNA and normalized to control cells; $n = 6$ independent experiments. (**F**) ABC immunolabeling in HCT116 cells with overexpression (APC) or silencing (siAPC) of the *APC* gene (β-catenin in green and nuclear staining in blue). Quantifications represent the means ± SD; $n = 3$ independent experiments for each condition. Original magnification, ×63. (**G**) Same as in **F**, with or without RIP140 overexpression. In each condition, data are expressed relative to controls without overexpression of RIP140. Mann-Whitney *U* test. $^*P < 0.05$; $^{**}P < 0.01$; $^{***}P < 0.001$.

with the inhibition of cell cycle progression by RIP140, we observed that tumors from RIP140-overexpressing HCT116 cells exhibited a strong and significant decrease in volume (2.5-fold) as compared with that of controls (Figure 4D). Sections of HCT-RIP xenografts stained with H&E showed large areas with faint eosin staining and lysed nuclei, which are usually associated with necrosis (Figure 4E). Such areas with karyolysis were significantly smaller in HCT-GFP tumors than those in the HCT-RIP tumors (14.4% ± 8.1% and 45.6% ± 19.1% of the whole tumor surface, respectively). Altogether, these data demonstrate that RIP140 inhibits colon cancer cell proliferation in vitro and tumor growth in vivo.

Effect of RIP140 on Wnt signaling in human colon cancer cells. To investigate whether the effect of RIP140 on human colon cancer cell proliferation was associated with an inhibition of β-catenin activation, we performed immunofluorescence staining to detect total and active (ABC) β-catenin in the two HCT116 cell lines, with some of the cells overexpressing RIP140. As noticed in mouse intestine, we observed no differences in the quantification of total β-catenin immunolabeling (Figure 5A left panel), but detected a 3-fold reduction of ABC staining in cells overexpressing RIP140 (Figure 5A right panel). As shown in Figure 5B, the regulation of dephosphorylated β-catenin expression by RIP140 was confirmed by Western blot experiments. As observed in mouse intestinal epithelium, this effect was associated with a decrease of several β-catenin target genes in HCT-RIP cells (Figure 5C). To more directly demonstrate regulation of the Wnt pathway by RIP140, we performed the classical TCF reporter assay by transiently transfecting the two reporter plasmids (pTOPflash or pFOPflash) into our stable HCT116 clones with or without RIP140 overexpression. As shown in Figure 5D (left panel), the level of β-catenin–driven transcription activity, measured as the TOP/FOP luciferase reporter ratio, was significantly lower in RIP140-overexpressing HCT116 cells (HCT-RIP) compared with that in control HCT116 cells (HCT-GFP). Finally, and as expected, an upregulation of the same Wnt reporter assays was detected in mouse embryonic fibroblasts (MEFs) isolated from *RIPKO* embryos compared with wild-type MEFs (Figure 5D, right panel). In order to strengthen these data, we analyzed the effect of siRNA-mediated depletion of RIP140 expression in human colon cancer cells. To this end, we used RKO colon cancer cells, which exhibit an intact Wnt/APC/β-catenin pathway. Interestingly, the knockdown of RIP140 expression in RKO cells (RKO-siRIP versus RKO-siCTL cells; Supplemental Figure 4A) led to an increase in ABC staining (Supplemental Figure 4B) and resulted in an increase of its target gene expression (Supplemental Figure 4C).

Altogether, these results demonstrate a clear inhibition of the Wnt/APC/β-catenin signaling pathway by RIP140. As shown in Supplemental Figure 4D, we assessed the impact of RIP140 on twelve Wnt target genes in both mouse gut and human colon cancer cells and found that a majority of these genes (more than 60% and 80%, respectively) were regulated by RIP140.

RIP140 increases transcription of the APC gene in human colon cancer cells. We then quantified the expression of members of the β-catenin degradation complex in the stable HCT116 clones with or without RIP140 overexpression. As shown in Figure 6A, the *APC* tumor suppressor gene was significantly upregulated by about 2-fold in HCT116 cells overexpressing RIP140. We also observed the specific deregulation of *APC* mRNA levels (2-fold decrease) after siRNA-mediated depletion of RIP140 expression in RKO cells (Figure 6B). Very few studies have examined the regulation of *APC* gene transcription. However, characterization of the proximal promoter region of the human *APC* gene identified functional consensus binding sites for several transcription factors including p53, USF1/2, and SP1 (refs. 26, 27, and Figure 6C). In order to demonstrate transcriptional regulation of the *APC* gene by RIP140, we transiently transfected HCT116 colon cancer cells with two reporter constructs containing the *APC* gene's proximal promoter region (encompassing sequences of 972 bp and 186 bp, respectively) fused to the luciferase coding sequence. As shown in Figure 6C, we observed a clear induction of luciferase activity upon cotransfection with a RIP140 expression vector, indicating that RIP140 was able to transactivate the *APC* gene promoter. This effect was specific, since control reporter vectors used in parallel were not affected by RIP140 overexpression (Figure 6C and ref. 28).

ChIP experiments were performed to demonstrate the presence of RIP140 on the proximal region of the *APC* promoter. PCR was performed in parallel on the proximal human *APC* promoter corresponding to the sequence that conferred regulation by RIP140 in the luciferase assays, on an upstream region (control), and on the *CCNE2* promoter (both used as negative controls). As shown in Figure 6D, we observed significant amplification of all three regions after anti-histone H3 ChIP. By contrast, we detected specific recruitment of RIP140 (as compared with the use of an irrelevant antibody only) on the *APC* promoter, thus identifying the *APC* gene as a direct transcriptional target of RIP140.

In order to demonstrate that regulation of APC was indeed required for regulation of β activation by RIP140, we used HCT116 cells with APC overexpression or depletion, as assessed by quantification of *APC* mRNA levels (Figure 6E), and observed regulation of ABC staining mainly after ectopic expression of APC (Figure 6F). Very interestingly, inhibition of ABC staining by RIP140 was lost when APC expression was modulated (Figure 6G), indicating that RIP140 activity was dependent on *APC* gene regulation.

To further support the role of APC in RIP140 activity in colon cancer cells, we used SW480 cells, which expressed a mutated form of APC (29) and stably engineered these cells to overexpress GFP-

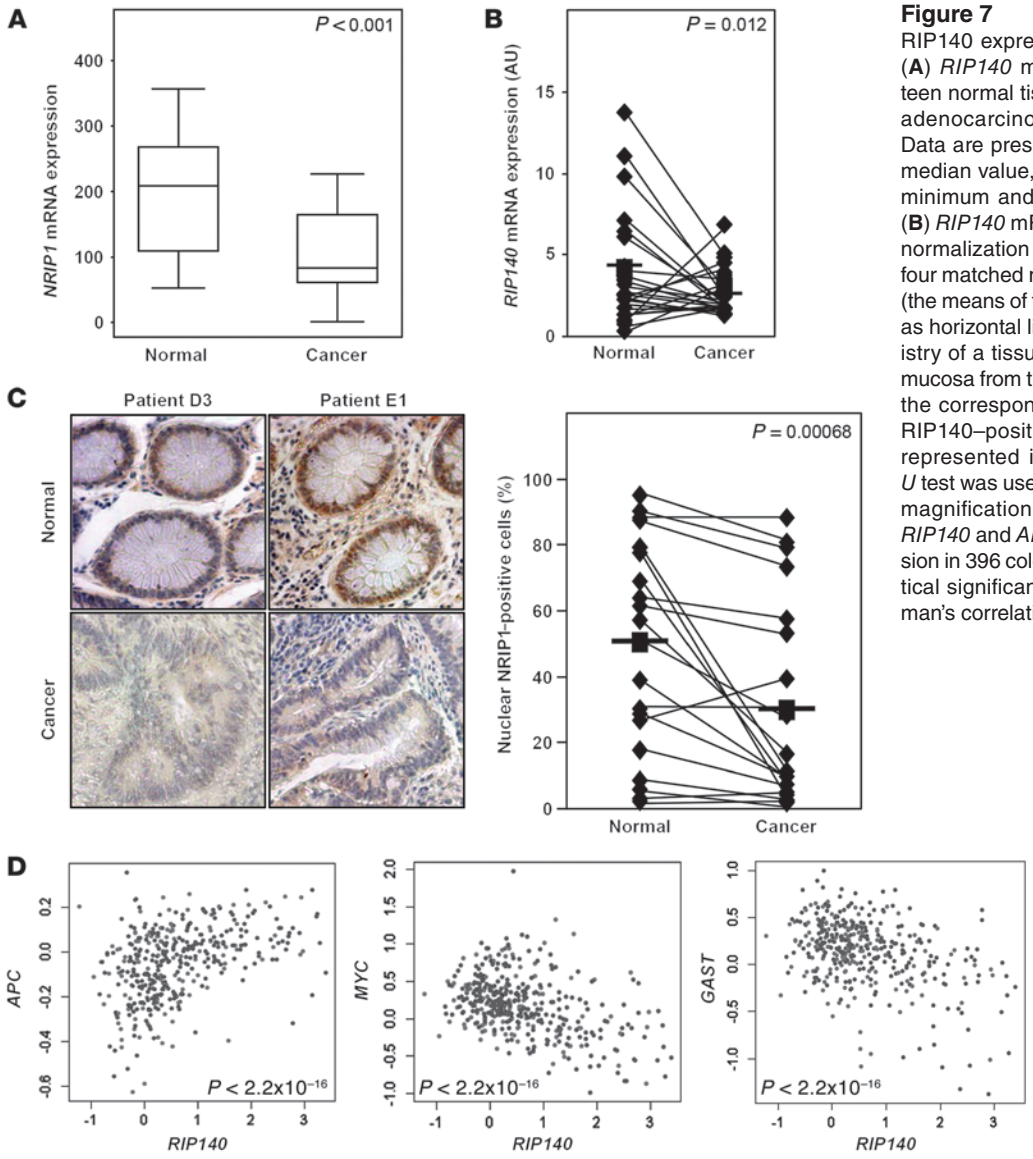

Figure 7
RIP140 expression in human colon cancers. (**A**) *RIP140* mRNA was quantified in seventeen normal tissues and twenty-two colorectal adenocarcinomas as previously described. Data are presented as box plots showing the median value, upper and lower quartiles, and minimum and maximum nonatypical values. (**B**) *RIP140* mRNA levels expressed in AU after normalization to actin mRNA levels in twenty-four matched normal and tumor colon samples (the means of the two populations are indicated as horizontal lines). (**C**) RIP140 immunochemistry of a tissue microarray containing normal mucosa from twenty-four patients together with the corresponding adenocarcinoma. Nuclear RIP140–positive cells were counted and are represented in a dot plot. A Mann-Whitney *U* test was used for statistical analysis. Original magnification, x10. (**D**) Correlation between *RIP140* and *APC*, *MYC*, or *GAST* gene expression in 396 colorectal adenocarcinomas. Statistical significance was assessed using Spearman's correlation analysis.

RIP140 (SW-RIP cells) or GFP alone (SW-GFP cells) (Supplemental Figure 5A). The effect of RIP140 overexpression on in vitro cell proliferation (Supplemental Figure 5B) and on tumor growth after xenografting (Supplemental Figure 5C) was significantly less intense in stably transfected SW480 cells as compared with its effect on HCT116 cells (Figure 4, B and C). The effect of RIP140 on β-catenin activation was also milder in SW480 cells than in HCT116 cells (Supplemental Figure 5D).

Decreased expression of the RIP140 gene in human colon cancers. To determine the biological relevance of our results in human pathology, we first quantified *RIP140* gene expression in human colon cancer samples as compared with that in normal colon tissues. First, we reanalyzed the published Affymetrix DNA microarray data on seventeen normal tissues and twenty-two colon cancers (30). As shown in Figure 7A, the results clearly revealed a significant decrease in *RIP140* mRNA levels in colon cancer biopsies. We confirmed these findings by real-time qPCR analysis of twenty-four pairs of normal colon and tumor colon tissue samples and found decreased *RIP140* expression in almost 60% of the tumors (Figure 7B).

In order to highlight the decreased *RIP140* gene expression in colon cancer, we performed immunohistochemical analysis using an anti-RIP140 antibody on a tissue microarray (TMA) containing twenty-four adenocarcinoma samples matched with the corresponding normal tissues. As observed at the mRNA level, we noticed a significant decrease in nuclear RIP140–positive cells in 60% of the colon adenocarcinomas as compared with those seen in normal tissues (Figure 7C).

We searched for a correlation between *RIP140* and *APC* gene expression in human colon biopsies. In perfect agreement with the data from mice and human colon cancer cell lines, the reanalysis of a transcriptomic study performed in a cohort of 396 colon cancers (31) revealed a very significant positive correlation between the expression of the two genes at the mRNA level (Figure 7D). We also assessed the correlation between APC and RIP140 expression in a subset of tumors with microsatellite instability that exhibit fewer losses or gains of chromosomal regions (32). In these tumors, the direct regulation of *APC* gene transcription by RIP140 should lead to a stronger correlation of their mRNA levels, since no LOH in chromosome 5q

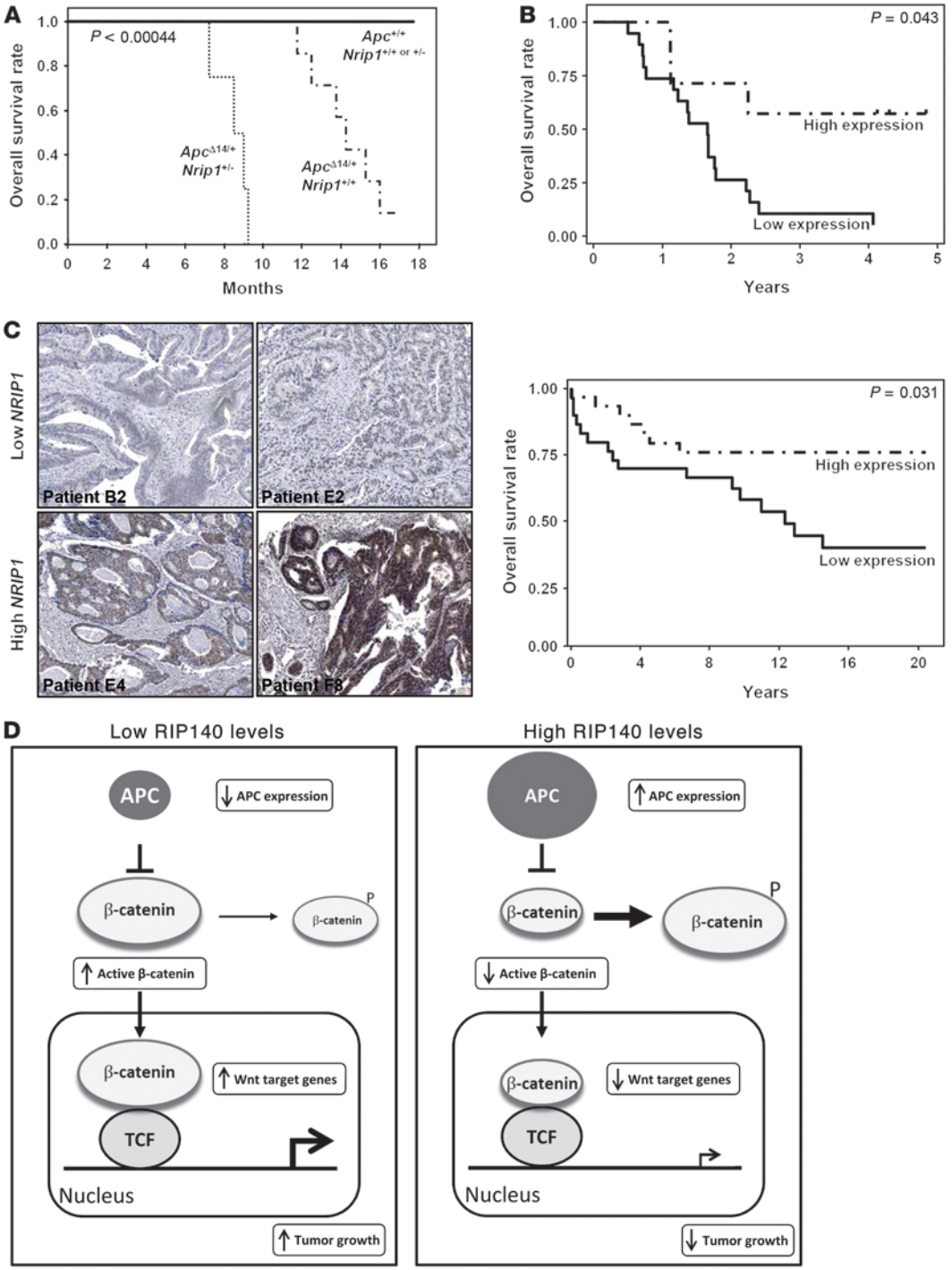

Figure 8

RIP140 is a prognosis marker in colon cancer. (**A**) Kaplan-Meier plots of cumulative survival of $Apc^{+/+}$, $Apc^{\Delta 14/+}$, and $Apc^{\Delta 14/+}$ $Rip140^{+/-}$ mice; $n = 4$ mice for the $Apc^{\Delta 14/+}$ $Rip140^{+/-}$ genotype and 6 mice for the $Apc^{+/+}$ and $Apc^{\Delta 14/+}$ genotypes. (**B**) Kaplan-Meier plots of OS of patients with tumors exhibiting low or high *RIP140* mRNA expression. (**C**) RIP140 immunochemistry of a tissue microarray containing adenocarcinomas from fifty-nine patients. Patients were ranked according to RIP140 expression in the tumor and divided into low and high RIP140 expression groups, respectively. Kaplan-Meier plot of the cumulative survival of patients with low or high *RIP140* gene expression. A log-rank test was used for statistical analysis. Original magnification, x10. (**D**) Schematic diagram depicting the role of RIP140 on β-catenin signaling in human colon cancer cells. RIP140 directly increases *APC* gene expression, which inhibits activation of β-catenin (RIP140 reduces levels of the unphosphorylated form of β-catenin). As a consequence of the drop in ABC levels, RIP140 inhibits Wnt target gene expression and decreases the ability of human colon cancer cells to proliferate and form tumors in nude mice.

would affect *APC* gene expression. As shown in Supplemental Figure 6, we found that the correlation between *APC* and *RIP140* expression was indeed stronger in microsatellite-unstable tumors (rho = 0.659) than in microsatellite-stable tumors (rho = 0.439). Finally, and as expected, RIP140 expression was inversely correlated with β-catenin target genes such as c-Myc (*MYC*) or gastrin (*GAST*) in the whole cohort (Figure 7D). Altogether, these data clearly demonstrate that colon tumorigenesis is associated with a decrease in RIP140 expression at both the mRNA and protein levels, a finding that is inversely correlated with the activation of Wnt signaling.

RIP140 expression as a prognostic marker in colon cancer. The results obtained in colon cancer cells and in patients led us to look for a link between RIP140 expression and colon cancer prognosis. As a first approach to demonstrate that low RIP140 expression levels in colon cancer could be associated with shorter survival, we used the *RIPKO* mouse model bred with the tumor-prone $Apc^{\Delta 14/+}$ mouse strain (5). These mice bear a germline invalidation of the *Apc* gene due to deletion of exon 14, which mimics human FAP in the severity of colon tumorigenesis. In this *Apc*-invalidated background, the loss of one *Rip140* allele strongly affected the lifespan of these mice. As shown in Figure 8A, Kaplan-Meier plots revealed that mice heterozygous for both the *Apc* and *Rip140* genes died earlier than $Apc^{\Delta 14/+}$ mice bearing the wild-type *Rip140* gene. These mouse experiments thus strongly supported the hypothesis that RIP140 expression could be associated with survival in colon cancer patients.

In support of this hypothesis, using the same set of tumors as in Figure 7A, we found that patients with high *RIP140* mRNA levels in the tumor presented better rates of overall survival (OS) than patients with low *RIP140* mRNA levels (Figure 8B). RIP140 expression was also found to be significantly correlated with progression-free survival (PFS) in two independent cohorts (Supplemental Figure 7, A and B). Moreover, as shown in Figure 8C, data obtained from labeling of a TMA containing fifty-nine adenocarcinoma samples indicated that OS rates were higher in patients bearing tumors with high RIP140 expression than in those with tumors expressing low levels of RIP140. Altogether, these results demonstrate that RIP140 expression decreases during colon tumorigenesis and is associated with poor patient survival.

Discussion

In the present study, we demonstrate that the transcriptional repressor RIP140 is involved in the regulation of intestinal epithelial homeostasis and tumorigenesis. Based on in vivo experiments using transgenic mice, our study first identified RIP140 as a new regulator of intestinal epithelial homeostasis through its significant impact on cell proliferation and apoptosis. Indeed, using both gain- and loss-of-function approaches, our data reveal that RIP140 strongly inhibits cell proliferation and programmed cell death in the intestinal epithelium. Our data also demonstrate that RIP140 plays an important role in colon cancer cells by inhibiting cell cycle progression and cell proliferation in vitro and in vivo after grafting onto nude mice.

Our work clearly demonstrates that RIP140 acts as a new inhibitor of the Wnt signaling pathway through the regulation of β-catenin activation (see Figure 8D). Indeed, RIP140 overexpression clearly inhibited the levels of ABC in both transgenic mice and in human colon cancer cells and tumor biopsies. This effect was observed by measuring the level of unphosphorylated ABC, by quantifying the expression of several β-catenin target genes, and by analyzing the regulation of a transiently transfected β-catenin–responsive reporter construct. Such regulation of the Wnt/APC/β-catenin signaling pathway by RIP140 could explain its effect on intestinal homeostasis and tumorigenesis, since many studies have demonstrated the importance of the Wnt pathway in controlling these processes. For instance, loss of APC function or altered β-catenin/TCF4 signaling in intestinal epithelium led to enhanced proliferation and apoptosis (33).

However, other nuclear signaling pathways targeted by RIP140, such as NRs (7) and E2Fs (8), could mediate some of the effects we observed. Indeed, several NRs exhibit a strongly deregulated expression in intestinal epithelium and have been shown to play an important physiopathological role in the intestine (34). For instance, receptors such as LRH-1 have promitotic activity, while others such as VDR, ER, and FXR play an antitumor role in mice (35). Some of these effects are mediated through regulation of the Wnt/APC/β-catenin signaling pathway by the corresponding NRs (36). By contrast, few data are available on the role of E2Fs in the intestine, although a recent study revealed that E2F4 determines cell cycle progression in normal intestinal epithelial crypt cells (37), while another study reported the role of Rb in the maintenance of enterocyte quiescence (38).

Interestingly, our work demonstrates that RIP140 directly induces transcription of the tumor suppressor *APC* gene. Indeed, RIP140 was recruited on the *APC* gene promoter and increased its transcription in transient transfection experiments. More importantly, RIP140 and APC expression was significantly correlated in mouse intestinal epithelium, in human colon cancer cell lines, and in human tumor biopsies. Although very few studies on the *APC* gene promoter have been published, several functional binding sites have been found in the human promoter sequence (26), and further work will be necessary to decipher the precise underlying molecular mechanisms.

Our data clearly indicate that the effects of RIP140 on β-catenin activation rely on the regulation of APC expression in human colon cancer cells. This observation could also be relevant in colon cancer cells bearing a mutation of the *APC* gene (see data on SW480 cells in Supplemental Figure 5) and is in line with a recent study demonstrating that truncated APC controls proliferation and β-catenin activity in colorectal cancer cell lines (39). However, more complex mechanisms could be implicated in physiological conditions. Indeed, in the mouse intestinal epithelium, we found that RIP140 regulated the expression of other members of the β-catenin destruction complex such as the *Csk1E* and *Axin2* genes. Positive regulation of the *Axin2* gene was surprising, since one would have expected the inhibition by RIP140 that occurs with other β-catenin target genes. This suggests that other transcription factors controlling expression of the *Axin2* gene are positively regulated by RIP140. Interestingly, the *Axin2* promoter encompasses a CG-rich region with Sp1 binding sites, which might support such a transcriptional increase in response to RIP140, as we previously reported for several promoters containing Sp1 binding sites (28).

Our results also demonstrate that RIP140 expression is finely regulated in both the normal and tumoral intestinal epithelia. The *RIP140* gene is expressed in epithelial cells, with stronger expression in differentiated cells of the villus than in proliferating cells of the crypt. The same gradient of *APC* gene expression was observed along the crypt/villus axis, where it counteracts β-catenin signaling and allows differentiation (40). We also showed that RIP140 expression (at both the mRNA and protein levels) strongly decreased during tumorigenesis. An attractive hypothesis to explain all of this regulatory activity is that RIP140 expression is negatively controlled by

the Wnt/APC/β-catenin pathway itself. Several negative transcriptional responses to activation of the Wnt/APC/β-catenin pathway have been reported (41), and a negative transcriptional element (sequence AGAWAW) has been identified in the promoter of the repressed genes (42). Bioinformatics analysis of the *RIP140* gene promoter identified two AGAWAW sites in the proximal region. The existence of such a transcriptional regulatory loop would explain the low *RIP140* gene expression in proliferating crypts and colon tumors, both of which exhibit constitutively high Wnt/APC/β-catenin activity, and might indicate that RIP140 expression must be tightly controlled to avoid deleterious effects on cells.

Finally, our work demonstrates that patients whose tumors contained high levels of RIP140 had better PFS and OS rates than those whose tumors had low RIP140 levels. Further studies are now required to define the clinical relevance of RIP140 as a prognostic marker compared with the previously reported gene signatures (43). These data, linking *RIP140* gene expression with patient survival, were supported by the decreased lifespan of mice bearing the $Apc^{\Delta 14/+}$ deletion associated with loss of one allele of the *Rip140* gene. It should be noted that during the crossing experiments, we did not obtain *Rip140*-null animals on an $Apc^{\Delta 14/+}$ background, suggesting that such double-transgenic animals are not viable. Altogether, our results strongly suggest that *RIP140* acts as a modifier gene of the APC-mutant phenotype in colon tumorigenesis. Indeed, it is now well known that although *APC* is considered the central gatekeeper gene in colon cancer, several genetic modifiers (such as the *Mom* genes for modifier of Min 1) have been identified and connect myriad factors that determine the course of the disease (for a review, see ref. 4). In vivo experiments using chemically induced carcinogenesis would also confirm the relevance of RIP140 in the initiation of colon tumorigenesis. A first experiment using azoxymethane and dextran sulfate sodium in *RIPKO* mice led to a stronger inflammatory response associated with histological abnormalities as compared with that in their wild-type littermates (data not shown). In line with all of these observations, a recent study performed in colon cancer samples by the Cancer Genome Atlas Network reported a mutation in the *RIP140* gene that encoded a truncated protein together with several nonsynonymous SNPs introducing amino acid changes in the RIP140 coding sequence (44). Interestingly, another frame shift mutation was previously reported in patients with familial colon cancers (45).

In summary, this study uncovers the role of RIP140 in intestinal homeostasis and colorectal carcinogenesis. In addition, these results identify RIP140 as a new regulator of *APC* gene transcription and as an inhibitor of the Wnt/APC/β-catenin pathway. Although several molecular events involved in tumor progression have been identified, the full sequence of steps leading to cancer is yet to be established. Our findings extend the knowledge of the role and mechanism of action of the *RIP140* gene at a molecular level and highlight, at a clinical level, the potential value of RIP140 as a biomarker with diagnostic, prognostic, and therapeutic utility in colon cancer.

Methods

Animals. C57BL/6J $Rip140^{-/-}$ (*RIPKO*) mice (12) were provided by M.G. Parker (Imperial College London). C57BL/6/129 *RIP140* transgenic (*RIPTg*) mice were generated using Speedy Mouse Technology (Nucleis) by insertion of a single copy of human *RIP140* cDNA at the *HPRT* locus. The coding sequence of the human *RIP140* gene (BclI/ClaI fragment) was cloned into the BamHI site of the Gateway pENTR-1A vector (Invitrogen) previously modified to include the rabbit β-globin polyA sequence and the *CAG* promoter. The transgene was then transferred into the pDEST-HPRT vector (Nucleis), which was linearized using AgeI and electroporated into HPRT-deficient BPES ES cells by standard methods. This construct contained two regions of homology with the *HPRT* gene, which allowed insertion of the transgene at this locus. The ES cell clones with homologous recombination were selected on hypoxanthine-aminopterin-thymidine–supplemented (HAT-supplemented) medium, and genotyping of HAT-resistant ES cell clones was performed by PCR analysis of genomic DNA using primers in the *RIP140* gene and in the poly (A) sequence (Supplemental Table 1). Targeted ES cells were injected into C57BL/6-derived blastocysts that were then transplanted into the uteri of recipient females. Resulting chimeric males were bred with C57BL/6 females, and the F1 agouti female offspring were backcrossed with C57BL/6 males. Animals were genotyped by qPCR using RIP140 primers. The tumor-prone $Apc^{\Delta 14/+}$ mouse strain was obtained from C. Perret (Institut Cochin, Paris, France) (5). These mice bear a germline invalidation of the *Apc* gene due to deletion of exon 14 and develop intestinal lesions mainly in the colon. All animals were maintained under standard conditions on a 12-hour light/12-hour dark cycle and were fed a chow diet ad libitum, according to European Union guidelines for the use of laboratory animals. In vivo experiments were performed on male and female mice in compliance with the French guidelines for experimental animal studies (agreement B34-172-27).

WBI. Twelve-week-old mice were anesthetized (i.p. injection of ketamine and xylazine), placed into a ventilated Plexiglas pie container, and underwent 12-Gy WBI using a Shephard 137Cs-ray irradiator at a dose rate of 4.21 Gy/minute. This was done according to the biosafety guidelines of the Val d'Aurelle hospital. Mice were killed 2.5 days after WBI, and small intestine was removed for histological analyses. The number and length of regenerating villi, together with the length of surviving crypts, were quantified (24 fields per genotype using ×10 magnification) in small intestine after H&E staining of paraffin sections (9 animals per group).

EdU detection in mouse tissues. Mice were injected i.p. with 100 to 200 μg of EdU (Invitrogen) in PBS. Small intestine was removed 2 hours after injection, paraformaldehyde fixed, paraffin embedded, and sectioned. After paraffin removal, sections were permeabilized with 0.5% Triton X100-PBS for 30 minutes at room temperature and then washed with 3% BSA-PBS. EdU incorporation was detected using the Click-iT EdU cell proliferation kit according to the manufacturer's instructions (Invitrogen). Following two rinses with PBS, slides were counterstained with Hoechst and mounted for fluorescence microscopy.

Real-time qPCR. Total RNA was extracted from cells or mouse tissues using the High Pure RNA Isolation kit (Roche Applied Science) according to the manufacturer's instructions. Sequential isolation of wild-type mouse small intestine epithelial cells was performed as described (46). Total RNA (1 μg) was subjected to reverse transcription using Superscript II reverse transcriptase (Invitrogen). Real-time qPCR was performed with the LightCycler 480 SYBR Green I Master (Roche Applied Science) and was carried out in a final volume of 10 μl using 0.25 μl of each primer (25 μM), 5 μl of the supplied enzyme mix, 2.5 μl of H_2O, and 2 μl of the template at a 1:10 dilution. After preincubation at 95°C, runs corresponded to 35 cycles of 15 seconds each at 95°C, 5 seconds at 60°C, and 15 seconds at 72°C. Melting curves of the PCR products were analyzed using LightCycler software to exclude amplification of nonspecific products. Results were normalized to *RS9* or *28S* housekeeping gene transcripts. See Supplemental Table 1 for the list of primer sequences.

ChIP analysis. For ChIP analysis, HCT116 cells (70% confluent) were cross-linked with 3.7% formaldehyde for 10 minutes at 37°C. The Champion ChIP One-Day Kit (QIAGEN) was then used according to the manufacturer's recommendations. Immunoprecipitations were performed using rabbit polyclonal antibodies against acylated-H3 (06-599; Upstate), RIP140 (Ab42126; Abcam), or an irrelevant IgG antibody as a control. qPCR was then performed using the LightCycler 480 SYBR Green I Master with 2 μl

of material per point. Primers flanking the RIP140 site of the *APC* promoter are listed in Supplemental Table 1. The input DNA fraction corresponded to 5% of the amount of immunoprecipitated chromatin.

Histological and immunofluorescence analyses. Mouse tissues were fixed with 4% paraformaldehyde, embedded in paraffin, and sectioned (5 μm). Histological analyses were performed by H&E staining of paraffin-embedded tissue sections. For immunofluorescence analysis, following incubation in citrate buffer solution, paraffin-embedded tissue sections were incubated with blocking serum for 3 hours to reduce nonspecific binding. Sections were then incubated with antibodies specific to RIP140 (Ab42126; Abcam), ABC (05-665, clone 8E7; Millipore), and total β-catenin (610153, clone 14; BD Transduction Laboratories). IF revelation was performed using an Alexa-conjugated secondary antibody (Invitrogen). After washing, sections were counterstained with Hoechst (Sigma-Aldrich) and mounted for fluorescence microscopy. Negative controls using rabbit or mouse IgGs were performed, and no staining was observed in these conditions. Staining quantification was performed at either ×20 or ×40 magnification (24 fields per genotype corresponding to 6 different animals) by determining the mean fluorescence intensity and staining area using the measurement and colocalization module available on AxioVision software, version 4.7.1 (Zeiss).

Cell culture and transfections. HCT116 human colon adenocarcinoma cells were stably transfected with the empty pEGFP vector (Clontech) or with the same vector containing full-length human *RIP140* cDNA (25). Pools of G418-resistant cells (respectively named HCT-GFP and HCT-RIP) were selected and grown in McCoy medium supplemented with 10% FCS, 100 U/ml penicillin, 100 mg/ml streptomycin, 100 mg/ml sodium pyruvate, and 750 μg/ml G418. To determine the fraction of cells in G1 and S phases, HCT116 cells were transiently transfected with cdt1-RFP using the Premo Fucci Cell Cycle Sensor (Invitrogen) and incubated with EdU (then detected as described above for mouse tissues). After fixation and mounting, Fucci and EdU fluorescent signals were quantified only in GFP- and GFP-RIP140–positive cells in order to determine the percentage of cells in G1 phase (Fucci-positive) and in S phase (EdU-positive). All transfections were carried out using Lipofectamine 2000 (Invitrogen) according to the manufacturer's instructions.

Luciferase assays. Stably transfected HCT116 cells and MEFs derived from wild-type or *RIPKO* mice (12) were transfected with the pTOPflash or pFOPflash reporter vectors and treated with or without Wnt3a-conditioned medium (47). HCT116 cells were transfected with an *APC* gene promoter reporter vector or with the same reporter plasmid bearing the *SV40* promoter together with a plasmid allowing RIP140 expression (pEF-c-myc-RIP140; ref. 48). Cells were plated in 96-well plates (3×10^4 cells per well) 24 hours prior to DNA transfection with Jet-PEI (200 ng of total DNA). The pRLCMVBis plasmid (Ozyme) was used to normalize transfection efficiency. Firefly luciferase values were measured and normalized to *Renilla* luciferase activity. For TOP/FOP assay, the values were expressed as the mean ratio of pTOPflash/pFOPflash luciferase activity.

Immunoblotting. After transfection, nuclear and cytoplasmic protein extracts were prepared using the NE-PER kit (Thermo Scientific), and cell extracts were analyzed by Western blotting using a primary antibody against RIP140 (Ab42125; Abcam), β-catenin (active or total), or β-actin (A2066; Sigma-Aldrich). Signals were revealed using a horseradish peroxidase–conjugated secondary antibody (Jackson ImmunoResearch) and enhanced chemiluminescence (ECL-Plus; GE Healthcare) according to the manufacturer's instructions.

Tumorigenicity assay. Six-week-old *nu/nu* female mice from Harlan, housed in a pathogen-free facility, were used to assess the effect of RIP140 on tumor growth. HCT-GFP and HCT-RIP cells (8×10^5 cells) were injected s.c., and tumor formation was monitored every 3 days using a caliper. Tumor volume was calculated as width × length × thickness. Mice were sacrificed 40 days after injection.

Cell proliferation assay. Stably transfected HCT116 cells (HCT-GFP and HCT RIP cells) were seeded at a density of 2,500 cells per well into E-Plate 16 (ACEA Biosciences, Inc.) containing 150 μl per well of medium supplemented with 10% FCS. Dynamic monitoring of cell growth was determined every 24 hours for 4 days using the impedance-based xCELLigence system (Roche Applied Science). The cell index was derived from measured cell-electrode impedance that correlates with the number of viable cells.

DNA microarray analysis. Published DNA microarray data (30, 31) were reanalyzed for *RIP140*, *APC*, *MYC*, and *GAST* expression. Optimal threshold values, which induced the best discrimination according to the disease progression status, were calculated to maximize the Youden's index. This index is defined as the sum of sensitivity and specificity minus 1 and is frequently used to dichotomize continuous variables in receiver operating characteristic (ROC) curve methodology.

TMAs. TMAs contained samples from twenty-four matched paraffin blocks from identified patients with primary colon cancer and adjacent normal tissue (T8235790d; Biochain) or from fifty-nine patients with adenocarcinoma (CD4; SuperBiochip). Three-micrometer sections of the TMA were deparaffinized and rehydrated in graded alcohol. Following epitope retrieval treatment in citrate buffer and neutralization of endogenous peroxidase, TMA sections were incubated overnight at 4°C with anti-RIP140 (Ab42126; Abcam). Immunohistochemical labeling was revealed using peroxydase-conjugated anti-rabbit secondary antibodies (Jackson ImmunoResearch) and 3,3′-diaminobenzidine (DAKO cytomation) as a substrate. Sections were counterstained with hematoxylin. Images were taken using NanoZoomer (Hamamatsu Photonics), and the percentage of stained nuclei was quantified using TissueQuest software (TissueGnostics).

Statistics. Data are presented as the means ± SD. Statistical comparisons were performed with Mann-Whitney *U* or Spearman's tests. Differences were considered statistically significant at a P value of less than 0.05. PFS was calculated from the start of palliative chemotherapy until disease progression or the last follow-up. Patients who died without progression were censored at the time of death. OS was calculated from the start of palliative chemotherapy until death. Patients lost to follow-up were censored at the time of last contact. The Kaplan-Meier method was used to estimate PFS and OS. The log-rank test was used to test the differences between groups that were considered statistically significant at a P value of less than 0.05. STATA statistical software (STATA) was used for all analyses. Additional methods are described in Supplemental Methods.

Acknowledgments

We thank the Réseau d'Histologie Expérimentale de Montpellier (RHEM) for histology facilities and F. Bernex for her expertise. We are grateful to J. Zilliacus (Karolinska Institutet Novum) for the gift of the pEGFP-C2-RIP140 vector; S. Narayan (University of Florida) for providing the APC reporter construct; P. Forgez (CdR Saint-Antoine) for the APC expression vector; and A. Coquelle (INSERM U896) for the Fucci/G1 plasmid. We also thank S. Fritsch for initial characterization of the *RIPTg* mice and C. Teyssier for critical reading of the manuscript. This work was supported by INSERM, Université de Montpellier 1, Fondation Lejeune, INCa (2011-054), SIRIC Montpellier, and the Institut Régional du Cancer de Montpellier (ICM).

Received for publication June 6, 2012, and accepted in revised form January 23, 2014.

Address correspondence to: Vincent Cavailles, IRCM, INSERM U896, 208 rue des Apothicaires, Montpellier F-34298, France. Phone: 33.4.67.61.24.05; Fax: 33.4.67.61.67.87; E-mail: vincent.cavailles@inserm.fr.

1. Schneikert J, Behrens J. The canonical Wnt signalling pathway and its APC partner in colon cancer development. *Gut*. 2007;56(3):417–425.
2. Klaus A, Birchmeier W. Wnt signalling and its impact on development and cancer. *Nat Rev Cancer*. 2008;8(5):387–398.
3. Zeng X, et al. A dual-kinase mechanism for Wnt co-receptor phosphorylation and activation. *Nature*. 2005;438(7069):873–877.
4. Kwong LN, Dove WF. APC and its modifiers in colon cancer. *Adv Exp Med Biol*. 2009;656:85–106.
5. Colnot S, et al. Colorectal cancers in a new mouse model of familial adenomatous polyposis: influence of genetic and environmental modifiers. *Lab Invest*. 2004;84(12):1619–1630.
6. Cavailles V, et al. Nuclear factor RIP140 modulates transcriptional activation by the estrogen receptor. *EMBO J*. 1995;14(15):3741–3751.
7. Augereau P, et al. The nuclear receptor transcriptional coregulator RIP140. *Nucl Recept Signal*. 2006;4:e024.
8. Docquier A, et al. The transcriptional coregulator RIP140 represses E2F1 activity and discriminates breast cancer subtypes. *Clin Cancer Res*. 2010; 16(11):2959–2970.
9. Christian M, Tullet JM, Parker MG. Characterization of four autonomous repression domains in the corepressor receptor interacting protein 140. *J Biol Chem*. 2004;279(15):15645–15651.
10. Yang X-J, Seto E. Lysine acetylation: codified crosstalk with other posttranslational modifications. *Mol Cell*. 2008;31(4):449–461.
11. Docquier A, et al. The RIP140 gene is a transcriptional target of E2F1. *PLoS One*. 2012;7(5):e35839.
12. White R, et al. The nuclear receptor co-repressor nrip1 (RIP140) is essential for female fertility. *Nat Med*. 2000;6(12):1368–1374.
13. Leonardsson G, et al. Nuclear receptor corepressor RIP140 regulates fat accumulation. *Proc Natl Acad Sci U S A*. 2004;101(22):8437–8442.
14. Duclot F, et al. Cognitive impairments in adult mice with constitutive inactivation of RIP140 gene expression. *Genes Brain Behav*. 2012;11(1):69–78.
15. Nautiyal J, et al. The transcriptional co-factor RIP140 regulates mammary gland development by promoting the generation of key mitogenic signals. *Development*. 2013;140(5):1079–1089.
16. Fritah A, Christian M, Parker MG. The metabolic coregulator RIP140: an update. *Am J Physiol Endocrinol Metab*. 2010;299(3):E335–E340.
17. Van der Flier LG, Clevers H. Stem cells, self-renewal, and differentiation in the intestinal epithelium. *Annu Rev Physiol*. 2009;71:241–260.
18. MacDonald BT, Tamai K, He X. Wnt/β-catenin signaling: components, mechanisms, and diseases. *Dev Cell*. 2009;17(1):9–26.
19. Tan CW, et al. Wnt signalling pathway parameters for mammalian cells. *PLoS One*. 2012;7(2):e31882.
20. Hlubek F, et al. Heterogeneous expression of Wnt/β-catenin target genes within colorectal cancer. *Int J Cancer*. 2007;121(9):1941–1948.
21. Kim TH, Xiong H, Zhang Z, Ren B. β-Catenin activates the growth factor endothelin-1 in colon cancer cells. *Oncogene*. 2005;24(4):597–604.
22. Rodilla V, et al. Jagged1 is the pathological link between Wnt and Notch pathways in colorectal cancer. *Proc Natl Acad Sci U S A*. 2009;106(15):6315–6320.
23. Mann B, et al. Target genes of β-catenin-T cell-factor/lymphoid-enhancer-factor signaling in human colorectal carcinomas. *Proc Natl Acad Sci U S A*. 1999;96(4):1603–1608.
24. Van Es JH, et al. Wnt signalling induces maturation of Paneth cells in intestinal crypts. *Nat Cell Biol*. 2005;7(4):381–386.
25. Zilliacus J, et al. Regulation of glucocorticoid receptor activity by 14–3-3-dependent intracellular relocalization of the corepressor RIP140. *Mol Endocrinol*. 2001;15(4):501–511.
26. Jaiswal AS, Balusu R, Narayan S. 7,12-Dimethylbenzanthracene-dependent transcriptional regulation of adenomatous polyposis coli (APC) gene expression in normal breast epithelial cells is mediated by GC-box binding protein Sp3. *Carcinogenesis*. 2006;27(2):252–261.
27. Jaiswal AS, Narayan S. Upstream stimulating factor-1 (USF1) and USF2 bind to and activate the promoter of the adenomatous polyposis coli (APC) tumor suppressor gene. *J Cell Biochem*. 2001; 81(2):262–277.
28. Castet A, et al. Receptor-interacting protein 140 differentially regulates estrogen receptor-related receptor transactivation depending on target genes. *Mol Endocrinol*. 2006;20(5):1035–1047.
29. Nishisho I, et al. Mutations of chromosome 5q21 genes in FAP and colorectal cancer patients. *Science*. 1991;253(5020):665–669.
30. Del Rio M, et al. Gene expression signature in advanced colorectal cancer patients select drugs and response for the use of leucovorin, fluorouracil, and irinotecan. *J Clin Oncol*. 2007;25(7):773–780.
31. Salazar R, et al. Gene expression signature to improve prognosis prediction of stage II and III colorectal cancer. *J Clin Oncol*. 2011;29(1):17–24.
32. Jass JR. Classification of colorectal cancer based on correlation of clinical, morphological and molecular features. *Histopathology*. 2007;50(1):113–130.
33. Sansom OJ, et al. Loss of Apc in vivo immediately perturbs Wnt signaling, differentiation, and migration. *Genes Dev*. 2004;18(12):1385–1390.
34. Modica S, et al. The intestinal nuclear receptor signature with epithelial localization patterns and expression modulation in tumors. *Gastroenterology*. 2010;138(2):636–648.
35. D'Errico I, Moschetta A. Nuclear receptors, intestinal architecture and colon cancer: an intriguing link. *Cell Mol Life Sci*. 2008;65(10):1523–1543.
36. Mulholland DJ, Dedhar S, Coetzee GA, Nelson CC. Interaction of nuclear receptors with the Wnt/β-catenin/Tcf signaling axis: Wnt you like to know? *Endocr Rev*. 2005;26(7):898–915.
37. Garneau H, Paquin M-C, Carrier JC, Rivard N. E2F4 expression is required for cell cycle progression of normal intestinal crypt cells and colorectal cancer cells. *J Cell Physiol*. 2009;221(2):350–358.
38. Guo J, Longshore S, Nair R, Warner BW. Retinoblastoma protein (pRb), but not p107 or p130, is required for maintenance of enterocyte quiescence and differentiation in small intestine. *J Biol Chem*. 2009;284(1):134–140.
39. Chandra SHV, Wacker I, Appelt UK, Behrens J, Schneikert J. A common role for various human truncated adenomatous polyposis coli isoforms in the control of β-catenin activity and cell proliferation. *PLoS One*. 2012;7(4):e34479.
40. Andreu P, et al. Crypt-restricted proliferation and commitment to the Paneth cell lineage following Apc loss in the mouse intestine. *Development*. 2005; 132(6):1443–1451.
41. Hoverter NP, Waterman ML. A Wnt-fall for gene regulation: repression. *Sci Signal*. 2008;1(39):pe43.
42. Blauwkamp TA, Chang MV, Cadigan KM. Novel TCF-binding sites specify transcriptional repression by Wnt signalling. *EMBO J*. 2008;27(10):1436–1446.
43. Nannini M, et al. Gene expression profiling in colorectal cancer using microarray technologies: results and perspectives. *Cancer Treat Rev*. 2009;35(3):201–209.
44. Cancer Genome Atlas Network. Comprehensive molecular characterization of human colon and rectal cancer. *Nature*. 2012;487(7407):330–337.
45. Mori Y, et al. Identification of genes uniquely involved in frequent microsatellite instability colon carcinogenesis by expression profiling combined with epigenetic scanning. *Cancer Res*. 2004; 64(7):2434–2438.
46. Weiser MM. Intestinal epithelial cell surface membrane glycoprotein synthesis. II. Glycosyltransferases and endogenous acceptors of the undifferentiated cell surface membrane. *J Biol Chem*. 1973;248(7):2542–2548.
47. Shibamoto S, et al. Cytoskeletal reorganization by soluble Wnt-3a protein signalling. *Genes Cells*. 1998;3(10):659–670.
48. Castet A, et al. Multiple domains of the receptor-interacting protein 140 contribute to transcription inhibition. *Nucleic Acids Res*. 2004;32(6):1957–1966.